Excited-State Proton Transfer of Equilenin and Dihydroequilenin: Interaction with Bilayer Vesicles†

Lesley Davenport,‡ Jay R. Knutson,§ and Ludwig Brand*

Biology Department and McCollum-Pratt Institute, The Johns Hopkins University, Baltimore, Maryland 21218

Received August 5, 1985

ABSTRACT: The two-state excited-state proton-transfer process for *d*-equilenin [*d*-3-hydroxyestra-1,3,-5(10),6,8-pentaen-17-one] and dihydroequilenin is found to depend both on pH and on proton acceptor concentration. Both the protonated and deprotonated forms of the excited molecule are fluorescent. As is the case for 2-naphthol, the excited-state pK_a (pK_a*) is substantially lower than the ground-state pK_a. Fluorescence decay studies have been performed as a function of emission wavelength in aqueous solutions at pH 6.9 in the presence of acetate anion (0.1 M). At this pH, both back-reaction from the excited-state and ground-state heterogeneity are minimal. A monoexponential decay is found in the blue region of the spectrum and a biexponential decay on the red edge. The lifetimes measured across both regions are constant, with a negative preexponential term, characteristic of an excited-state reaction, evident at longer wavelengths. Decay-associated spectra (DAS), the preexponential terms associated with the measured lifetimes, have been acquired for these aqueous solutions. Equilenin and dihydroequilenin are found to adsorb to dimyristoyllecithin (DML) vesicles. Rates for excited-state proton transfer are greatly reduced when dihydroequilenin adsorbs to vesicles. The accessibility of the bound probe to acetate as a proton acceptor depends on the cholesterol content of the vesicles.

Aromatic alcohols exhibit excited-state ionization constants that differ by several orders of magnitude from those observed for the ground state (Förster, 1949a,b; Weller, 1961; Ireland & Wyatt, 1976). Nanosecond time-resolved fluorescence measurements may provide the rates for interconversion of the excited, protonated, and ionized species and the rates for their depopulation to the ground state (Birks, 1970; Laws & Brand, 1979). These rates depend on the character of the fluorophore and on the nature of the surrounding milieu such as pH, polarity, viscosity, and the presence of proton donors and acceptors.

The following describes steady-state and nanosecond time-resolved studies of equilenin and dihydroequilenin, both in solution and in the presence of dimyristoyllecithin single bilayer vesicles. These fluorescent estrogens have spectral properties similar to those of naphthol (Bates & Cohen, 1950; Slaunwhite et al., 1951; Weinreb et al., 1974, 1977) with proton loss from the 3′-position (Figure 1). Although the kinetics of the excited-state proton-transfer reaction for naphthol in aqueous solutions has been studied in great depth (Weller, 1955, 1958a,b), less information is available for the corresponding excited-state reaction of equilenin and dihydroequilenin.

We have used fluorescence decay studies to obtain decay-associated spectra (DAS).[1] These have revealed differences between the decay processes of equilenin and dihydroequilenin.

When dihydroequilenin is adsorbed to vesicles, the rate of excited-state proton transfer is greatly reduced. The accessibility of the bound probe to acetate as a proton acceptor is further found to depend on the cholesterol content of the vesicles. A preliminary account of this work has appeared elsewhere (Davenport et al., 1983).

Theory

The kinetic scheme for the reversible two-state excited-state reaction shown below is described by eq 1 and 2 under the boundary conditions [B*] = 0 at $t = 0$ (only A is directly excited):

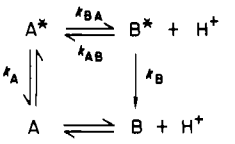

$$I_A(\lambda,t) = [A^*]_0 S_A(\lambda)\frac{k_{FA}(\gamma_2 - X)}{\gamma_2 - \gamma_1}(e^{-t/\tau_1} + Ae^{-t/\tau_2}) \quad (1)$$

$$I_B(\lambda,t) = [A^*]_0 S_B(\lambda)\frac{k_{FB}k_{BA}}{\gamma_2 - \gamma_1}(e^{-t/\tau_1} - e^{-t/\tau_2}) \quad (2)$$

where $[A^*]_0$ = initial concentration of A* produced by a δ excitation function, $A = (X - \gamma_1)/(\gamma_2 - X)$, $X = k_A + k_{BA}$, $Y = k_B + k_{AB}[H^+]$, and γ_1 and $\gamma_2 = \tau_1^{-1}$ and $\tau_2^{-1} = (1/2)\{(X + Y) \pm [(Y - X)^2 + 4k_{BA}k_{AB}[H^+]]^{1/2}\}$. k_{FB} and k_{FA} are emission rates of the respective species. Equations 1 and 2 can be reexpressed as

$$I_A(t) = \alpha_1 e^{-t/\tau_1} + \alpha_2 e^{-t/\tau_2} \quad (3)$$

$$I_B(t) = \beta_1 e^{-t/\tau_1} + \beta_2 e^{-t/\tau_2} \quad (4)$$

The fluorescence decay times τ_1 and τ_2 are identical for emission from both species, and the preexponential terms

† This work was supported by National Institutes of Health Grant GM 11632. This is Contribution No. 1300 from the McCollum-Pratt Institute.

‡ Present address: Chemistry Department, The City University of New York, Brooklyn College, Brooklyn, NY 11210.

§ Present address: Laboratory of Technical Development, NHLBI, National Institutes of Health, Bethesda, MD 20205.

[1] Abbreviations: DAS, decay-associated spectra; *d*-dihydroequilenin, *d*-estra-1,3,5(10),6,8-pentaene-3,17β-diol; DML, L-α-dimyristoyllecithin; EDTA, ethylenediaminetetraacetic acid; *d*-equilenin, *d*-3-hydroxyestra-1,3,5(10),6,8-pentaen-17-one; TLC, thin-layer chromatography; TRES, time-resolved emission spectra.

0006-2960/86/0425-1186$01.50/0

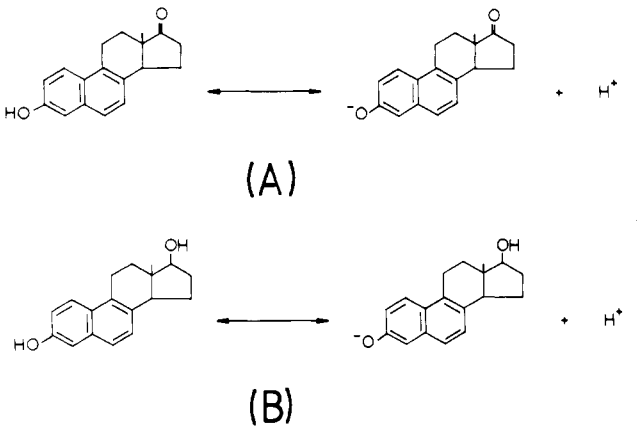

FIGURE 1: Structures of the protonated and deprotonated forms of (A) *d*-equilenin and (B) dihydroequilenin.

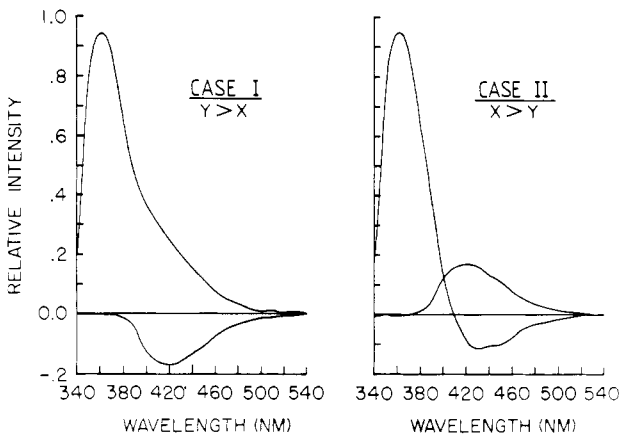

FIGURE 2: Simulated decay-associated spectra describing two kinetic mechanisms for depletion from the A* and B* states, under irreversible reaction conditions. The decay-associated spectra are defined as the preexponential terms for a given fluorescence lifetime as a function of the emission wavelength. In case I, the combined rate constant Y describing depletion processes from the B* state is greater in magnitude than X ($Y > X$), the combined rate constant for depletion from the A* state. This leads to the characteristic decay-associated spectra shown, with a zero contribution from the shorter lifetime component in the A* region of the spectrum; i.e., monoexponentiality at shorter wavelengths is implied. In case II, the decay-associated spectra reflect the kinetic mechanism where $X > Y$. Such a mechanism is inferred from fluorescence studies of β-naphthol. Under these conditions, the longer lifetime component is zero in the A* region of the spectrum. For both models, the negative preexponential term is associated with the shorter lifetime component.

describing the decay of the B* state are equal in magnitude and opposite in sign. As may be expected, the lifetimes and preexponential terms show a strong pH dependence (Laws & Brand, 1979). With increasing pH, above the excited-state pK_a, the reaction becomes irreversible ($K_{AB}[H^+] \rightarrow 0$ as $[H^+] \rightarrow 0$). The initial boundary conditions remain valid in this region, provided there is no effective ground-state heterogeneity ($[B]_0 = 0$). The preexponential terms simplify in this region such that one of the components (α_1 or α_2) tends to zero. The relative magnitudes of the combined rate constants X and Y determine which preexponential tends to zero. In either case, monoexponentiality for the decay of A* is implied by irreversibility.

The preexponential terms depend on the rate constants describing the excited-state processes. Consider two complementary mechanistic situations: First, when deactivation from the A* state proceeds faster than that from the B* state, whether by radiative or nonradiative processes, the combined rate constant X exceeds Y and (under irreversible reaction conditions) $\alpha_1 = 0$ and β_2 is negative. In the complementary case, the kinetic relationship is reversed; i.e., $Y > X$. In this irreversible case, $\alpha_2 = 0$ and β_2 is again negative in character. For both mechanisms, the negative preexponential term observed on the red edge of the emission spectrum is *always* associated with the *shorter* lifetime component. The total fluorescence emission envelope can be separated into the product of a wavelength $[S(\lambda)]$ and a time distribution (Knutson et al., 1982):

$$I_A(\lambda,t) = S_A(\lambda)[\alpha_1 e^{-t/\tau_1} + \alpha_2 e^{-t/\tau_2}] \quad (5)$$

$$I_B(\lambda,t) = S_B(\lambda)[\beta_1 e^{-t/\tau_1} + \beta_2 e^{-t/\tau_2}] \quad (6)$$

Measurement of decay-associated spectra, DAS (defined here as the preexponential terms associated with a given lifetime across the emission wavelength region), provides an indication of the kinetic mechanism for that two-state reaction. The DAS for the alternate models described above are contrasted in Figure 2. The expected decay-associated spectra are signatory in each case. The DAS represent spectral distributions of the excited-state emitting species (A and B) contributing to the total fluorescence at a particular wavelength and thus will contain contributions from both $S_A(\lambda)$ and $S_B(\lambda)$:

$$S_1 = \alpha_1 S_A(\lambda) + \beta_1 S_B(\lambda) \quad (7)$$

$$S_2 = \alpha_2 S_A(\lambda) + \beta_2 S_B(\lambda) \quad (8)$$

When $\alpha_1 = 0$ ($X > Y$), the DAS recovered for τ_1, the longer lifetime component, will correspond to the spectral shape associated with the B* species. It is of interest to note that for the alternate case ($Y > X$ and $\alpha_2 = 0$) the derived DAS will be the inverse B* spectrum, arising directly from the negative preexponential terms (Figure 2).

Methods to obtain decay-associated spectra (DAS) have been described elsewhere (Knutson et al., 1982). Time-resolved emission spectra (TRES) obtained over two different time windows provide sufficient information to resolve two decay-associated spectra. The emission in each time window, in convolved space, is a mixture of the constituent spectra from each species $[S_{A,B}(\lambda)]$ with an appropriate mixing coefficient, C_i. The correct mixing coefficients are defined as the integral, within the time window $a \rightarrow b$, of the observed exponential decay component D_i:

$$C_i(a \rightarrow b) = \int_a^b D_i(t')\, dt' \quad (9)$$

Here D_i is the observed response decay function corresponding to the convolution of the impulse response function d_i, with an excitation profile $L(t)$ of

$$D(t') = \int_0^{t'} L(t) d_i(t'-t)\, dt \quad (10)$$

Hence, the mixed spectrum obtained for the time window $a \rightarrow b$ can be expressed as

$$I'(\lambda,a \rightarrow b) = \sum S_i(\lambda) C_i(a \rightarrow b) \quad (11)$$

For the two-state excited-state process discussed here, the experimentally obtained TRES collected from time windows $a \rightarrow b$ and $c \rightarrow d$ are defined by

$$I'(\lambda,a \rightarrow b) = S_1(\lambda)C_1(a \rightarrow b) + S_2(\lambda)C_2(a \rightarrow b) \quad (12)$$

$$I'(\lambda,c \rightarrow d) = S_1(\lambda)C_1(c \rightarrow d) + S_2(\lambda)C_2(c \rightarrow d) \quad (13)$$

$I'(\lambda,a \rightarrow b)$ and $I'(\lambda,c \rightarrow d)$ are the spectra obtained by summing all photon counts between instrument channels $a \rightarrow b$ and $c \rightarrow d$, respectively. $C_1(a \rightarrow b)$ and $C_2(a \rightarrow b)$ are the mixing coefficients for components 1 and 2, respectively. They

are defined as the integrals under the convolved *monoexponential* decay profiles for decays 1 and 2, respectively, over the time interval $a \rightarrow b$. The same process is used to obtain coefficients for time window $c \rightarrow d$. Since TRES are obtained in convolved space, it follows that it is also necessary to obtain the mixing coefficients in convolved space. To calculate the lifetime DAS S_i, one first inverts the matrix of mixing coefficients (**C**). Then $\vec{S} = \mathbf{C}^{-1} \cdot \vec{T}$, where $\vec{T}$ are the TRES in the different windows and $\vec{S}$ are the different DAS.

The lifetime DAS [$S_1(\lambda)$ and $S_2(\lambda)$] derived from windowed TRES must be recombined if one is interested in the *species* spectra. The inversion of eq 7 and 8 yields

$$S_A(\lambda) = [\beta_2 S_1(\lambda) - \beta_1 S_2(\lambda)]/(\alpha_1\beta_2 - \alpha_2\beta_1) \quad (14)$$

$$S_B(\lambda) = [\alpha_2 S_1(\lambda) - \alpha_1 S_2(\lambda)]/(\alpha_2\beta_1 - \alpha_1\beta_2) \quad (15)$$

In the homogeneous case mentioned above, $|\beta_1| = |\beta_2|$, so all β terms can be removed from eq 14. S_A is just proportional to the sum of S_1 and S_2. In the irreversible case, one of the α's will null, further simplifying eq 15 to yield S_1 or S_2. In the more general case, knowledge of the coefficients (α_i, β_i) can always produce species DAS (or SAS) from the lifetime DAS, $S_i(\lambda)$. Depending on the system, one may obtain the needed coefficients via changes in solution conditions (i.e., to overdetermine rate parameters) or by suitable assumptions about boundary conditions (as described above).

The procedure for extraction of SAS described above can be summarized in matrix notation:

$$\vec{S} = \mathbf{C}^{-1} \cdot \vec{T} \quad (16)$$

$$\vec{S}' = \mathbf{M} \cdot \vec{S} \quad (17)$$

where $\vec{T}$ are experimental TRES, S are lifetime DAS, **C** is a matrix of mixing coefficients (eq 14 and 15), and $\vec{S}'$ is the desired species DAS (or SAS).

M, the DAS $\rightarrow$ SAS mixing matrix (eq 14 and 15, using the column index summing convention), is given by

$$\begin{bmatrix} \dfrac{\beta_2}{\beta_2\alpha_1 - \beta_1\alpha_2} & \dfrac{-\beta_1}{\beta_2\alpha_1 - \beta_1\alpha_2} \\ \dfrac{\alpha_2}{\alpha_2\beta_1 - \alpha_1\beta_2} & \dfrac{-\alpha_1}{\alpha_2\beta_1 - \alpha_1\beta_2} \end{bmatrix} \quad (18)$$

When both steps are combined, it is clear that SAS may be obtained directly from the TRES:

$$\vec{S}' = \mathbf{M} \cdot \mathbf{C}^{-1} \cdot \vec{T} = \mathbf{N} \cdot \vec{T} \quad (19)$$

The TRES $\rightarrow$ SAS mixing matrix **N** can be derived from the product **M**·**C**. Alternatively, **N** can be obtained from integration of the windowed areas under the *biexponential* convolved A* and B* decay functions (eq 3 and 4). For either approach, determination of the α_1/α_2 and/or β_1/β_2 ratios is necessary. Procedures for global analysis in terms of rate constants for excited-state reactions and SAS have also been developed (Beechem et al., 1984, 1985). They have distinct advantages both in the evaluation of confidence limits and in making simple extensions to study more complex phenomena.

Experimental Procedures

Materials and Methods. Equilenin, L-α-dimyristoyllecithin (DML), and cholesterol were purchased from Sigma Chemical Co. Dihydroequilenin was supplied by Steraloids Inc. The compounds were used without further purification. Purity of the compounds was verified by TLC on silica gel plates (Eastman Chromatogram) with chloroform–methanol–aqueous ammonia (100:15:1 by volume) and chloroform–methanol–water (65:25:4 by volume) as the developing solvent for the steroid-like molecules and phospholipid, respectively. Spot identification was by phosphorus staining reagent (Dittmer & Lester, 1964) for the phospholipid and by charring (2% methanol in H_2SO_4, by volume) for the steroids. Sodium acetate (anhydrous powder) was purchased from J. T. Baker Chemical Co. 2-Naphthol was purified as described in detail elsewhere (Loken et al., 1972).

Solutions of equilenin and dihydroequilenin (4×10^{-6} M) in deionized water were prepared by dilution of a 1 mM stock solution (in ethanol) into water. HCl and NaOH were used to adjust the pH. The pH of the samples was allowed to equilibrate for about 8 h before measurements were made. All fluorescence studies were carried out at 15 ± 1 °C with fully aerated samples. For samples containing acetate, a 2 M stock solution was prepared and the pH adjusted to 6.9 before passing it through a Millipore filter (Millex-GS, 0.22 μm, Millipore). Serial dilutions of this stock were made.

DML and DML/cholesterol single bilayer vesicles were prepared in 0.1 M NaCl, pH 6.9, with 1 mM EDTA at 30 °C by sonication under argon, to minimize lipid peroxidation (Hauser et al., 1971; Brunner et al., 1976). Fractionation of vesicles was achieved by ultracentrifugation above the phospholipid phase transition temperature (Beckmann airfuge) at 100000g for 60 min according to the method of Barenholz et al. (1977). The concentration of phospholipid was determined from lipid phosphorus content (McClare et al., 1971). Labeling of vesicles with equilenin or dihydroequilenin (1 mM in ethanol) was achieved by direct injection of small aliquots of the stock solution into a vortexing suspension of vesicles to give the required phospholipid to fluorescent probe labeling ratio.

Fluorescence Spectroscopy Measurements. Steady-state fluorescence measurements were performed on a Perkin-Elmer MPF4 spectrofluorometer as described in detail elsewhere (Chen et al., 1977). A quarter wave plate was used in the excitation path to obviate any polarization bias. Fluorescence emission spectra were collected under appropriate "magic angle" emission conditions (Spencer & Weber, 1970). No further corrections were made for instrument response. Samples were excited at 337 nm with excitation and emission bandwidths of 4 nm each. The absorbance of all fluorescence samples was less than 0.1 at the wavelength of excitation, in order to reduce inner filter effects (Parker & Rees, 1962).

Steady-state emission anisotropy was measured on the Perkin-Elmer MPF4, by selecting appropriate polarizations in both the excitation and emission beams with polarizers mounted between the cuvette and the focusing and collecting lenses, respectively. The steady-state emission anisotropy $\langle r \rangle$ was calculated from

$$\langle r \rangle = \frac{GI_{VV} - I_{VH}}{GI_{VV} + 2I_{VH}} \quad (20)$$

where $G = I_{HH}/I_{HV}$ and represents a correction factor for the inequality of sensitivity of the detection system to horizontally and vertically polarized emission (Azumi & McGlynn, 1962; Chen & Bowman, 1965; Paoletti & LePecq, 1969).

Nanosecond time-resolved fluorescence decay studies were performed in a single photon counting fluorometer described elsewhere (Badea & Brand, 1979). Fluorescence decay curves were collected contemporaneously with a light scatter profile. The excitation wavelength was isolated with a Baird Atomic 3400-Å interference filter. The exciting light passed through a scrambler plate, and the fluorescence was measured through a polarizer oriented at 54.7° to the horizontal plane. The fluorescence emission passed through a Bausch and Lomb

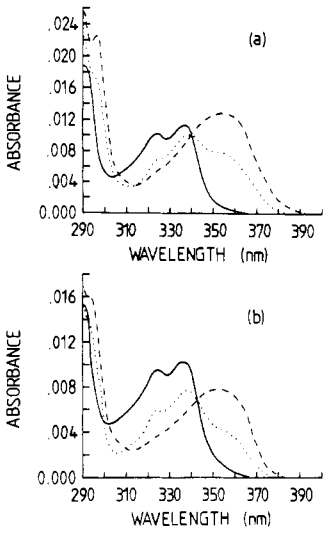

FIGURE 3: Absorption spectra for aqueous (a) equilenin and (b) dihydroequilenin (4.1×10^{-6} M) as a function of pH: fully protonated form, (—) pH 1.57 ± 0.01 and (···) pH 9.62 ± 0.01, respectively, and (--) fully ionized form, pH 12.14 and 12.02, respectively (bandwidth 0.8 nm).

0.5-m monochromator, operated under computer control. Excitation and emission bandwidths of 13 nm were used.

9-Cyanoanthracene in HPLC-grade methanol and 2-naphthol in water at pH <1 were used as monoexponential standards to verify functioning of the instrument and to correct for the wavelength-dependent transit time of the photomultiplier. Data analysis was done by the method of nonlinear least squares (Knight & Selinger, 1971; Grinvald & Steinberg, 1974).

Collection of Decay-Associated Spectra. (*A*) *DAS from TRES.* Time-windowed fluorescence emission spectra (TRES) (Easter et al., 1976) were collected as described in detail elsewhere (Knutson et al., 1982). A "time window" was established by summing the photon counts over a given group of channels on the time axis for each experimental decay profile. These brief decay curves (20-s dwell times) were collected as a function of the emission wavelength. This was achieved by stepping the emission monochromator at 1-nm intervals through the wavelength region of interest. The photon counts collected within each time window were summed and stored within the computer memory. The "channel-summing" window method allows all of the windowed TRES to be collected simultaneously.

(*B*) *Global DAS Procedure.* Mini fluorescence decay curves were collected across the emission wavelength region of interest (350–560 nm), by stepping the emission monochromator in increments of 2 nm. A dwell time of 4 min each on the two sample positions was used, with a 30-s dwell on the lamp position. One sample contained a monoexponentially decaying standard, from which the wavelength-dependent shifts were determined. The excitation wavelength, bandwidths, and optics were identical with those described above. The three-dimensional decay surface obtained was analyzed by a global nonlinear least-squares fitting procedure (Knutson et al., 1983; Beechem et al., 1985). The two decay constants were linked across the decay surface, and the derived preexponential terms represent the DAS for each decay term.

RESULTS

Fluorescence in Solution. With increasing pH, the absorption spectra for aqueous solutions of *d*-equilenin and dihydroequilenin (Figure 3) reveal a shift to longer wavelengths

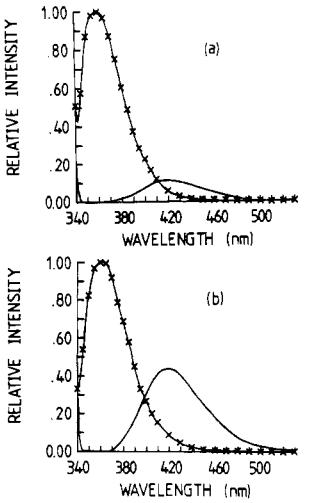

FIGURE 4: Steady-state fluorescence emission spectra of aqueous (a) equilenin and (b) dihydroequilenin (4.1×10^{-6} M) at pH 1.57 ± 0.01 (×) and at pH 12.08 ± 0.06 (—). Excitation was at 337 nm, with excitation and emission bandwidths of 4 nm each, respectively. Temperature was 15 °C.

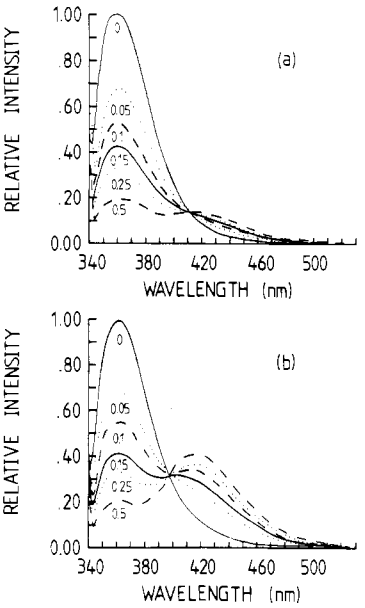

FIGURE 5: Steady-state fluorescence emission spectra for aqueous (a) equilenin and (b) dihydroequilenin at pH 6.9 (4.1×10^{-6} M) titrated with sodium acetate. The spectra were measured at the following acetate concentrations: (—) zero, (···) 0.05 M, (--) 0.1 M, (—) 0.15 M, (···) 0.25 M, and (--) 0.5 M. The excitation wavelength was 337 nm with excitation and emission bandwidths of 4 nm each, respectively. The temperature was 15 °C.

and the appearance of a broad featureless spectrum with peak absorbance near 355 nm at alkaline pH. This corresponds to the absorbance of the fully ionized form. An isosbestic point is observed at 342 nm. An absorption titration (360 nm) for both compounds gave results in accord with the Henderson–Hasselbalch relation, with a pK_a close to that found for 2-naphthol (Weller, 1961).

The fluorescence spectra of equilenin and dihydroequilenin in the protonated and ionized forms are shown in Figure 4. The fluorescence spectra of both compounds, at neutral pH, in the absence and presence of acetate are shown in Figure 5. In the absence of acetate, little emission due to the ionized form is evident. This can be explained by the fact that the excited-state proton transfer is kinetically limited. In the presence of acetate as a proton acceptor, the excited-state process is described by eq 21, and as shown in Figure 5, a

Table I: Fluorescence Decay Parameters for Equilenin (pH 6.9, 0.1 M Acetate)

λ_{em} (nm)	τ_1	α_1	τ_2	α_2	χ^2
360	3.5	0.47			1.4
440	3.6	0.75	1.4	−0.58	1.5

contribution of emission of the ionized species to the steady-state fluorescence spectrum becomes evident:

$$A^* + R^- \underset{k_2}{\overset{k_1}{\rightleftharpoons}} B^* + RH \qquad (21)$$

Hence, $k_{AB}^{app} = k_{AB}[H^+] + k_2[RH]$ and $k_{BA}^{app} = k_{BA} + k_1[R^-]$.

Fluorescence decay measurements of equilenin and dihydroequilenin were carried out in the presence of acetate. The decay parameters found for equilenin at neutral pH in the presence of 0.1 M acetate are given in Table I. Under these conditions the decay from A* (isolated at 360 nm) is essentially a monoexponential. The decay constant is 3.5 ns. As will be shown below, this lifetime may be assigned to X (2.7×10^8 s^{-1}). At 440 nm, a biexponential decay becomes apparent with the addition of a short decay time with a negative amplitude. Global analysis (Knutson et al., 1983) of the 360- and 440-nm decay sets with linkage of decay times does reveal a small contribution of the short decay time at 360 nm. Since the protonated species also contributes to the emission at 440 nm, the two amplitudes are not equal in magnitude. At this pH, the concentration of ground-state B is negligible.

Decay-associated spectra were obtained by two different methods. DAS were extracted from TRES with the procedure of Knutson et al. (1982) (1-nm intervals, 20 s per step). These were obtained over broad "early" and "late" time intervals. We selected early and late time windows in a convenient manner. When the convolved decay curve for the long component (3.6 ns) is integrated in the intervals, the boundaries can be chosen to make early and late areas equal. Thus, extraction of the derived DAS (Figure 6a) for the other component is achieved by simple subtraction of the late TRES from the early TRES. The 1.4-ns DAS (Figure 6a) is essentially zero over the 350–380-nm (A* emission) wavelength region as predicted for an irreversible excited-state reaction (eq 7 and 8; with $\alpha_2 \rightarrow 0$). The negative character of this DAS is in accord with the existence of an excited-state proton-transfer reaction. Comparison of this DAS with the simulated DAS shown in Figure 2 indicates that equilenin is described by model I. Deactivation of the B* state (k_B) proceeds faster than from the A* state; i.e., $Y > X$.

Windowed TRES, used above to calculate DAS, do not contain all of the details of the time dependence in the surface (intensity vs. wavelength and time). Rather, they are condensed sections of the surface that can be stored easily for future study. As computer resources became available, however, we stored the entire decay surface. Decay curves (Figure 7) for aqueous equilenin and dihydroequilenin at pH 6.9, 0.1 M acetate, were obtained at 2-nm intervals over the emission wavelength region 350–550 nm. The decay surfaces were analyzed by a global procedure (Knutson et al., 1983; Beechem et al., 1985) with the two decay constants linked across the decay surface. The derived preexponential terms provide the DAS.

Figure 6b shows the DAS for equilenin. Both long and short decay components are in essential agreement with the DAS (from TRES) of Figure 6a. Figure 6c shows the DAS (from global analysis alone) for dihydroequilenin under identical conditions. As mentioned under Theory, the ratio of total rates depopulating A* (X) to those depopulating B* (Y) determines which lifetime will contribute in the A* spectral region. In

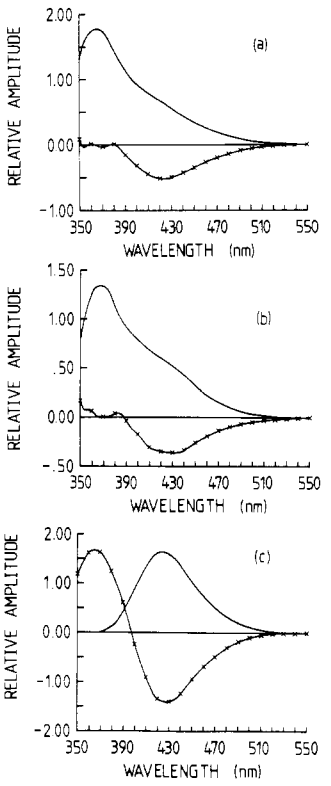

FIGURE 6: Decay-associated fluorescence emission spectra (DAS) for (a) aqueous equilenin at pH 6.9 containing 0.1 M acetate, by the window method. The DAS (preexponential) of the short-decay component (×) was obtained by subtraction of the late-windowed from the early-windowed TRES. The DAS associated with the long-decay component (—) was obtained from the late-windowed TRES, minus a small multiple of the early-windowed TRES (see text). Amplitudes of (b) equilenin and (c) dihydroequilenin, obtained from the global DAS procedure. For both molecules, the short- (×) decay component (1.9 ns for equilenin and 4.5 ns for dihydroequilenin) is associated with the negative preexponential term; the long-lifetime component (—) was determined to be 3.5 ns for equilenin and 8.3 ns for dihydroequilenin. Excitation was 337 nm, with excitation and emission bandwidths of 13 nm each, respectively. Temperature was 15 °C. Global χ^2 values were 0.93 and 1.03 for equilenin and dihydroequilenin, respectively.

contrast with equilenin, dihydroequilenin shows a short lifetime feature in this blue region, while its longer lifetime amplitude vanishes. This is due to the inequality $X > Y$ for dihydroequilenin, as compared with $Y > X$ for equilenin. In this regard, dihydroequilenin is similar to the parent molecule 2-naphthol (Laws & Brand, 1979). The negative DAS will always be associated with the short decay constant. This can be understood in the following way. The total emission due to B* must be positive ($\beta_1\tau_1 + \beta_2\tau_2$). Thus, the decay time associated with the negative amplitude (β) must always be smaller than that associated with the positive amplitude.

As indicated by eq 5, the preexponential terms for the decay of B* are equal in magnitude and opposite in sign, provided only A is excited. This mirror image relationship is clearly evident over the long-wavelength regions of Figure 6. The A* spectral contribution appears in the long-lifetime DAS in Figure 6b (equilenin) and in the short-lifetime DAS in Figure 6c (dihydroequilenin). In addition, the relative contribution of B* is larger for dihydroequilenin than for equilenin.

In the case of ground-state heterogeneity, lifetime DAS represent the spectra of the individual species in the mixture. As has been indicated above, this is not the case for an excited-state reaction. Rather, the decay function for each species contains both the lifetimes, and the DAS for each decay constant contains spectral contributions from both the species

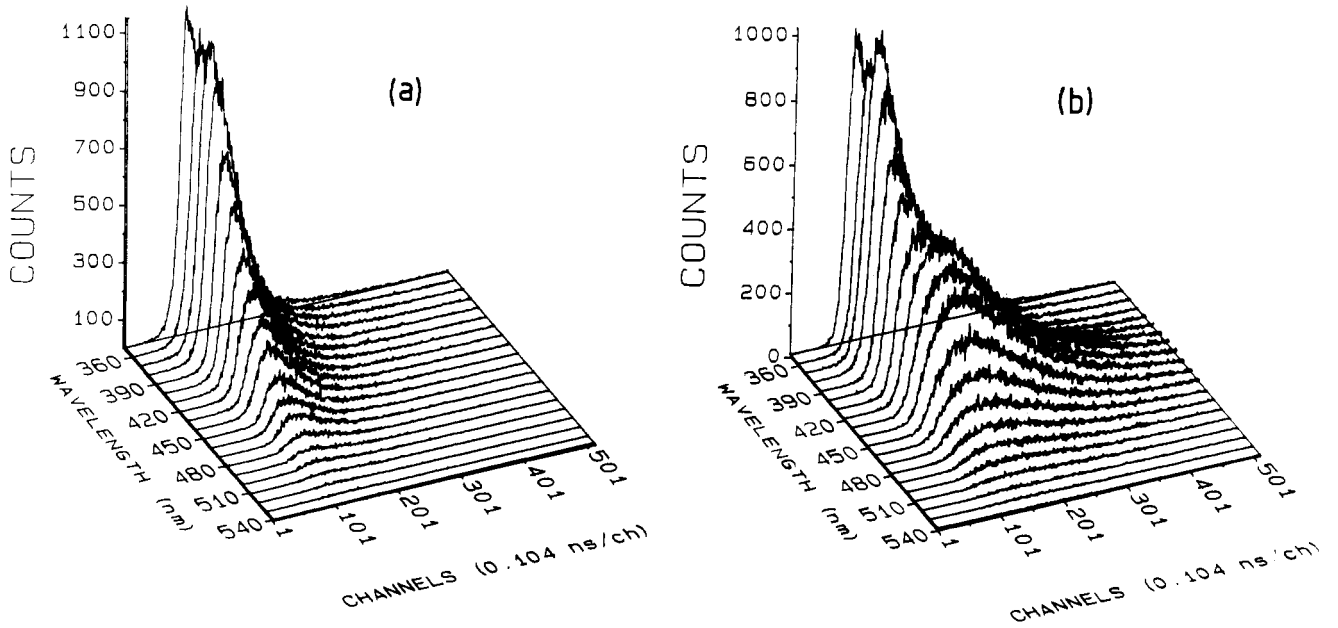

FIGURE 7: Fluorescence decay curves for aqueous (a) equilenin and (b) dihydroequilenin containing 0.1 M acetate, pH 6.9 at 15 °C. The data were collected at 2-nm intervals across the emission wavelength range (shown every 10 nm here for clarity). The data collection time at each wavelength was 4 min. The excitation wavelength was 337 nm with excitation and emission bandwidths of 13 nm each, respectively (0.104 ns/channel). The enhanced fluorescence yield of the B* species for dihydroequilenin as compared to equilenin observed at longer emission wavelengths is clearly seen. The rise time (resulting from the negative preexponential factor) is also evident at red-shifted wavelengths.

(Figure 6). Without additional information or assumptions about boundary conditions or rates, these DAS and their lifetimes represent the maximum information available. For the system under study, further information is in fact available.

The emission spectra for each *species* (species DAS or SAS) are readily obtained from the DAS and are shown in panel a (equilenin) and panel b (dihydroequilenin) of Figure 8. In these irreversible cases with excitation solely into A, eq 14 and 15 are simplified, since either α_1 or α_2 must vanish and $|\beta_1| = |\beta_2|$. For either case, the SAS for the A* species is simply the sum of the two lifetime DAS. In this irreversible case, the SAS for the B* species appears directly as one of the two lifetime DAS. For the equilenin case, it is the inverse of the short lifetime DAS, while in the dihydroequilenin case it is given directly by the longer lifetime DAS. It is of interest to point out that the DAS that corresponds to the B* SAS is invariably associated with the lifetime that would be obtained by direct excitation of B*. In the more general case, full knowledge of the α and β terms for eq 14 and 15 is required to generate the SAS. These terms can be obtained from experiments that perturb the rates (Laws & Brand, 1979) or by extrapolation into, or isolation of, pure spectral regions. Alternatively, global analysis can be used to obtain SAS (Beechem et al., 1985). In this study, we have not separated the X and Y values into their respective rate constants (k_A, k_B, k_{BA}, k_{AB}) since this cannot be done without perturbation of the system. Both inverse plots (Laws & Brand, 1979) and SAS (Beechem et al., 1985d) require a change in solution conditions (or special assumptions) to subdivide these rates. Since one cannot be certain of the benign nature of these changes with respect to membrane structure, we chose to extract the maximum information available from the unperturbed system. As excited-state reaction/SAS techniques develop further, perhaps by incorporating absorption data (R. P. DeToma, personal communication) and/or by constraining SAS to be everywhere positive, the task of subdividing X and Y will simplify.

Interaction with Vesicles. Studies have been performed on the interaction of equilenin and dihydroequilenin with single

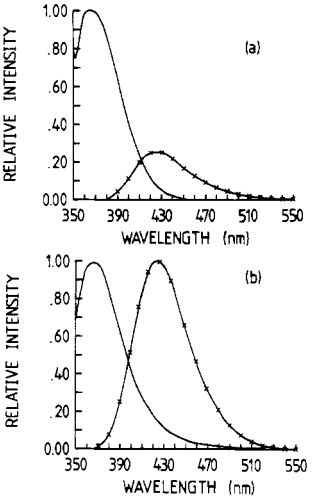

FIGURE 8: Species-associated spectra (SAS) for (a) equilenin and (b) dihydroequilenin. For an irreversible excited-state reaction, the SAS for the A* species (—) is simply the sum of the two lifetime DAS. The SAS for the B* species appears directly from the lifetime DAS, after normalization of the β terms.

bilayer DML vesicles. On addition of the estrogens to the bilayer, the value of the steady-state emission anisotropy is observed to increase from zero in 0.1 M NaCl, to ~0.12 at 15 °C in the bilayer (labeling ratio 1:500, estrogen to phospholipid). Further evidence for interaction of the estrogens with the bilayer arises from measurement of the steady-state emission anisotropy as a function of increasing temperature. Figure 9 indicates that the probe rotational motions are sensitive to the physical state of the bilayer. The emission anisotropy decreases through the phase transition region of the bilayer. It appears that these probes may be located near the alkyl chain region of the bilayer. Probes located at the polar head group region generally show less dramatic changes through the phospholipid phase transition (Davenport, 1981).

Additional information about the interaction of the probes with the lipid bilayers is presented in Figure 10, which shows

Table II: Time-Resolved Decay Parameters of Dihydroequilenin[a]

sample	λ_{em}	α_1	τ_1	α_2	τ_2	α_3	τ_3	α_4	τ_4	χ^2
aqueous[b]	360	0.38	2.74	0.004	6.5					1.3[f]
	440[d]	−0.60	2.74	0.66	6.5					1.3[f]
vesicles[c]	360[e]	0.15	2.58	0.14	10.46					1.56[g]
	440[e]	−0.25	2.61	0.30	9.4					1.4[g]
	440[e]	−0.27	2.77	0.55	6.61	−0.53	6.77	0.31	9.43	1.38[g]

[a] The data were analyzed as a sum of exponential fits with a scatter component. The scatter was never greater than 5% of the total fluorescence signal. [b] Dihydroequilenin in 0.25 M acetate (4×10^{-6} M), pH 6.9. [c] DML vesicles labeled with dihydroequilenin 1:50 (probe to phospholipid molar labeling ratio). [d] Global analysis. [e] Single curve analysis. [f] Global χ^2. [g] χ^2 "local" for single curve analysis.

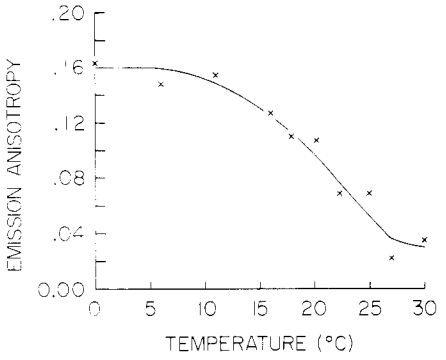

FIGURE 9: Steady-state emission anisotropy as a function of temperature for equilenin incorporated into DML vesicles. A molar labeling ratio of probe to phospholipid of 1:500 was employed. Excitation was at 337 nm, emission was at 360 nm, and excitation and emission bandwidths of 4 nm each, respectively, were used.

the effect of adding increasing amounts of acetate to DML (in 0.1 M NaCl at pH 6.9) labeled 1:50 (probe:phospholipid) with equilenin (panel a) and dihydroequilenin (panel b). When compared to the acetate effect in aqueous solution (cf. Figure 5), the facilitated transfer process for bilayer probes is suppressed. In addition, a saturation (absent in the solution data) is observed for the acetate effect in the DML vesicles. This suggests that these samples may contain a heterogeneous population of free (accessible) and bound (less accessible) probes.

Additional experiments were performed with dihydroequilenin. This molecule, as shown above, shows a significantly enhanced yield of the B* species in the presence of acetate. Evidence for coexistence of free and bound probe is shown in Figure 11, which gives steady-state emission anisotropy values as a function of increasing dihydroequilenin concentrations. A decreasing trend in the anisotropy is observed, which may be expected since the emission anisotropy is an intensity weighted average of those molecules free in solution ($\langle r \rangle \simeq 0$) together with those molecules bound to the bilayer. It appears that, as the ratio of probe to vesicles is increased, the fraction of fluorescence due to free dye also increases.

The fluorescence decay behavior of dihydroequilenin is indicated in Table II. The decay parameters found for the probe in 0.25 M acetate, pH 6.9, are characteristic of an essentially irreversible two-state excited-state reaction with $X > Y$ (τ_1 = 2.7 ns or $X = 3.7 \times 10^8$ s^{-1} and τ_2 = 6.5 ns or $Y = 1.5 \times 10^8$ s^{-1}). This B* decay can be contrasted with the value of 1.4 ns for τ_2 ($Y = 7.2 \times 10^8$ s^{-1}) found for equilenin. The results obtained for dihydroequilenin in the presence of DML single bilayer vesicles (Table II, bottom) are more difficult to interpret. Biexponential fits were not entirely adequate, yet little improvement was found with a fit to four exponential terms. The data presented in Figure 11 suggest that at the 1:50 labeling ratio up to half the dihydroequilenin is free in solution. This is in accord with the biexponential analysis

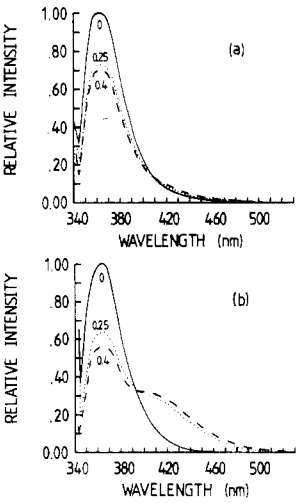

FIGURE 10: Steady-state fluorescence emission spectra for (a) equilenin- and (b) dihydroequilenin-labeled DML vesicles at pH 6.9 (molar labeling ratio 1:50; probe to phospholipid) as a function of increasing acetate concentrations: (—) zero, (···) 0.25 M, and (– –) 0.4 M. The excitation wavelength was 337 nm with excitation and emission bandwidths of 4 nm each, respectively. The temperature was 15 °C. The background signal from vesicle scatter was subtracted by using an unlabeled vesicle sample.

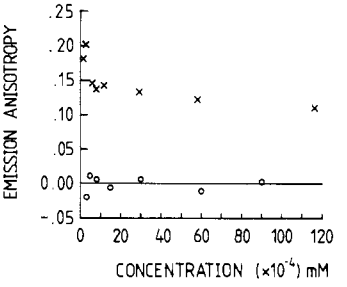

FIGURE 11: Steady-state emission anisotropy as a function of increasing dihydroequilenin concentration. The DML concentration was 0.58 mM. Polarized signals were corrected for vesicle scatter by subtraction of the appropriate polarized background intensities. The temperature was 15 °C with excitation and emission at 337 and 360 nm, respectively. Bandwidths of 8 and 12 nm, respectively, were employed.

shown in Table II. The decay constant of 2.6 ns seen at 360 nm may be easily assigned to free probe. This also appears at 440 nm with a negative preexponential. The ~10-ns decay (360 nm) might then be assigned to bound probe.

The result of a four-component fit to the decay data at 440 nm is also shown in Table II. This may be explained in the following way. τ_1 with its negative amplitude is assigned to $1/X$ ($X = k_A + k_{AB}$) for the free probe and τ_2 is assigned to $1/Y$ ($Y = k_B$ as $[H^+] \rightarrow 0$) for the free probe, in reasonable agreement with the aqueous data shown in Table II. τ_3 (with its negative amplitude) is $1/Y$ of the bound probe, then, while τ_4 is assigned to $1/X$ of the bound probe. Considering the nearly complementary amplitudes and lifetimes for components 2 and 3, it is not surprising that the simple biexponential

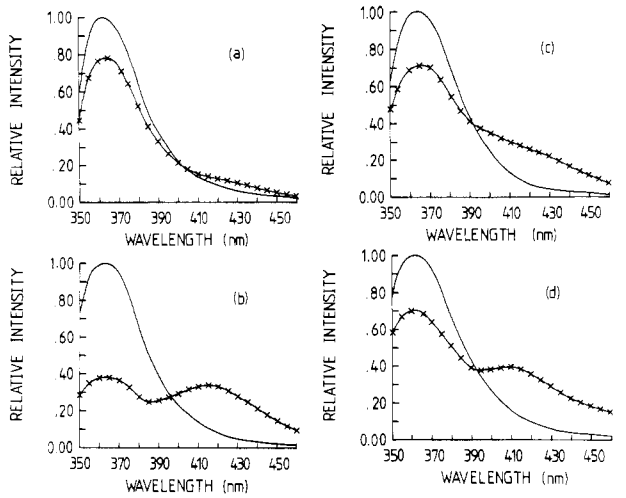

FIGURE 12: Steady-state fluorescence emission spectra for dihydroequilenin incorporated into (a) DML vesicles (0.58 mM) (molar labeling ratio 1:2000) and (b) 0.1 M NaCl, pH 6.9 (1.25×10^{-7} M); (c) DML vesicles at pH 6.9, containing 10 mol % cholesterol (molar labeling ratio 1:2864, probe to total lipid) and (d) 20 mol % cholesterol (molar labeling ratio 1:2424, probe to total lipid) in the absence (—) and presence (×) of 0.25 M acetate. Excitation was 337 nm, with excitation and emission bandwidths of 4 nm each, respectively. The temperature was 15 °C. Background vesicle scatter has been subtracted.

analysis gives an equally good fit. While the above may well represent an overinterpretation of the data, it does provide a self-consistent picture. In addition, it addresses the heterogeneity known to exist in the system. Further studies using multiple labeling ratios will be required to provide a fuller interpretation.

Subsequent steady-state fluorescence studies of the proton-transfer process of dihydroequilenin bound to the bilayer vesicles were performed with labeling ratios of 1:2000 (probe:phospholipid). Emission anisotropy values indicate a more complete binding of the dihydroequilenin at these low probe to vesicle ratios. The emission anisotropy values at 360 nm and 15 °C (Figure 11) were 0.11 (1:50), 0.14 (1:500), and 0.20 (1:2000) at the indicated probe to phospholipid ratios.

Figure 12a shows the effect of addition of 0.25 M acetate to dihydroequilenin-labeled DML vesicles (1:2000) at 15 °C, pH 6.9. The acetate enhancement in the red region of the emission spectrum, arising from formation of the deprotonated (B*) species in the excited state, is severely reduced compared to the effect of 0.25 M acetate on dihydroequilenin free in solution (Figure 12b). It appears that the majority of the dihydroequilenin molecules are buried within the bilayer architecture and are shielded from interaction with aceate anion. Several other (more lipophilic) proton acceptors such as triethylamine, dicyclohexylamine, and diallylamine were investigated (data not shown) and were found to quench the fluorescence of the protonated (A*) form, without producing a detectable B* emission. Single bilayer vesicles prepared from phosphatidylserine, having a net negative charge at pH 6.9, were not detectably different with respect to the dihydroequilenin. The probe is presumably buried in the interfacial region of the bilayer and is not significantly perturbed by changing the charged head group of the phospholipid.

As indicated above, the ability of acetate to facilitate proton transfer of dihydroequilenin is greatly reduced when the probe is incorporated into pure DML bilayer vesicles. Figure 12c,d shows the contrasting effect of acetate on the proton-transfer process of dihydroequilenin incorporated into DML vesicles containing 10 mol % (panel a) and 20 mol % (panel b) cholesterol. An enhanced accessibility to acetate is observed. Further, higher cholesterol concentrations yield a greater effect. An effective quenching of the A* species is observed at 360 nm in the presence of 0.25 M acetate. An increase in the yield of the B* species is observed at longer wavelengths. That a substantial amount of the fluorescence at 420 nm (B* region) is attributed to bound probe, rather than free, is indicated by the retension of relatively high emission anisotropy values (Table III; 0.13 at 10 mol % cholesterol and 0.10 with 20 mol % cholesterol at 420 nm).

Table III: Steady-State Emission Anisotropy Values of Cholesterol-Containing Vesicles at Two Emission Wavelengths

	no cholesterol		10 mol % cholesterol		20 mol % cholesterol	
	360 nm	420 nm	360 nm	420 nm	360 nm	420 nm
no acetate	0.16		0.19		0.19	
0.25 M acetate	0.15	0.14	0.23	0.13	0.23	0.10

DISCUSSION

We have exploited the multidimensional character of fluorescence spectroscopy to examine the luminescence properties of equilenin and dihydroequilenin free in solution and in the presence of single bilayer dimyristoyllecithin vesicles. The results described here indicate that, under proton-transfer conditions, there are significant differences between the luminescence properties of these two probes.

Fluorescence decay curves were obtained as a function of emission wavelength, and the data are presented in several different ways, each of which is advantageous in revealing some aspect of the fluorescence behavior of these probes. Typical decay curves obtained directly with the pulse fluorometer are shown in Figure 6. Time-resolved emission spectra (TRES) represent a time slice through this surface. TRES are a version of the original data, which may sometimes reveal heterogeneity or the presence of an excited-state reaction. Lifetime decay-associated spectra (DAS) as shown in Figure 7 are a derived form of the original data. In the case of ground-state heterogeneity, these DAS directly represent the emission spectra of each component in the mixture. For excited-state reactions, the one to one relationship between lifetime DAS and species breaks down. As has been shown here, these spectra are still useful in identifying the kinetic relationships in the system. The DAS for equilenin and dihydroequilenin in acetate shown in Figure 6b,c are diagnostic for two contrasting kinetic flows. The DAS directly reflect differences in depletion processes from the protonated and deprotonated species. For equilenin, $Y > X$ (X and Y are the combined rate constants for the depletion of the A* and B* species, respectively). For dihydroequilenin, ($X >$ Y), the A* species decays faster than the B* species.

Species-associated spectra (SAS) were also obtained for this system. They are in agreement with the known spectra of A* and B* obtained at extreme pH conditions.

While used here for a particular bimolecular reaction (with proton loss or gain), the TRES, DAS, and SAS framework can extend to a variety of other reactions in luminescence. Intermolecular energy-transfer processes, for example, are almost always irreversible and will be simple to resolve into donor/acceptor SAS. A similar applicability holds for the excimer and exciplex problems. Davenport et al. (1985) have used this same approach to resolve a complex heterogeneous system of intramolecular excimers in membranes. It is likely that many spectral problems previously grouped under "solvent relaxation" and studied with continuous models will yield

discrete states when studied with DAS and global analysis tools. These states and spectra should link to physically meaningful species.

Molecules that exhibit excited-state proton transfer are becoming of increasing importance for the study of biological microenvironments (DeLuca et al., 1971, Bowie & DeLuca, 1972, Loken et al., 1972; Örstan et al., 1986). Light-driven proton pulse experiments (Gutman, 1983) have been used to study the rates of protonation of defined proton acceptors located on the interface of micelles. The studies described here reveal that, on adsorption of equilenin or dihydroequilenin to the bilayer, these molecules are shielded from acetate anion, resulting in little proton transfer. Similar shielding effects have been observed for 2-naphthol intercalated into detergent micelles (Selinger, 1983). With addition of cholesterol to the bilayer, dihydroequilenin shows evidence of enhanced excited-state proton transfer, the effect increasing with increased cholesterol content. That the addition of cholesterol to the bilayer is not simply reducing the adsorbed fraction of dihydroequilenin is evidenced by the relatively high emission anisotropy values measured in both the A* *and* B* regions. The results presented here suggest that the ability of dihydroequilenin to selectively undergo proton transfer in the presence of cholesterol may serve as a probe for perturbation of membrane architecture. Previous studies (employing a variety of physical techniques) using model lipid membranes reveal strong evidence for "phase separation" involving cholesterol. It is likely that dihydroequilenin, a probe retaining steroidal character, may preferentially partition into cholesterol-rich regions, where the 3′-hydroxyl group may be exposed to external ionic species. Alternatively, cholesterol may disrupt the overall bilayer architecture, resulting in a "looser packing" of phospholipid molecules and increased vesicle diameter (Huang, 1969; Newman & Huang, 1975). This may cause dihydroequilenin to be more accessible to acceptors.

In the present study, a probe was selected for kinetic flows amenable to perturbation by acetate anion. The probe so selected was found to react quite differently in homogeneous and cholesterol-mixed bilayers, opening the possibility that the domain structure in lipids can be probed. In this regard, it is useful to note that ground-state (i.e., absorption) indicators of pH cannot yield the kind of dynamic information presented here. The fluorophore signal is sensitive not only to the equilibrium process of deprotonation but also to the *dynamic* availability of nearby acceptor (or donor) groups. This nanosecond "buffering capacity" measurement appears to be sensitive to the detailed structure of the lipid bilayer and may find use in studies of other macromolecules.

ACKNOWLEDGMENTS

We thank Drs. W. R. Laws, J. B. A. Ross, A. Örstan, and R. E. Dale for helpful discussions. We also thank Joseph M. Beechem both for valuable discussions and for the use of global analysis programs. We thank Mark D. Pritt for providing the three-dimensional plotting routine. We are grateful also to D. G. Walbridge for continued advice and technical assistance, together with Hazel Ward and Julie Kang for their patience in the preparation of the manuscript. We thank H. Ward for graphic arts assistance.

Registry No. Equilenin, 517-09-9; DML, 18194-24-6; cholesterol, 57-88-5; dihydroequilenin, 1423-97-8.

REFERENCES

Azumi, T., & McGlynn, S. P. (1962) *J. Chem. Phys. 37*, 2413–2420.

Badea, M. G., & Brand, L. (1979) *Methods Enzymol. 75*, 378.

Barenholz, Y., Gibbes, D., Litman, B. J., Goll, J., Thompson, T. E., & Carlson, F. D. (1977) *Biochemistry 16*, 2806–2810.

Bates, R. W., & Cohen, H. (1950) *Endocrinology (Philadelphia) 47*, 182.

Beechem, J. M., Knutson, J. R., Ross, J. B. A., Turner, B. W., & Brand, L. (1983) *Biochemistry 22*, 6054–6058.

Beechem, J. M., Ameloot, M., DeToma, R. P., & Brand, L. (1985a) *Biophys. J. 47*, 318a.

Beechem, J. M., Ameloot, M., & Brand, L. (1985b) *Chem. Phys. Lett. 120*, 466–472.

Beechem, J. M., Ameloot, M., & Brand, L. (1985c) in *Excited-State Probes in Biochemistry and Biology* (Masotti, L., & Szabo, A. G., Eds.) Plenum, New York (in press).

Beechem, J. M., Ameloot, M., & Brand, L. (1985d) *Anal. Instrum. (N.Y.)* (in press).

Birks, J. B. (1970) *Photophysics of Aromatic Molecules*, p 304, Wiley, New York.

Bowie, L., Irvin, R., & DeLuca, M. (1972) *Fed. Proc., Fed. Am. Soc. Exp. Biol. 31*, 420 (Abstr.).

Brunner, J., Skrabal, P., & Hauser, H. (1976) *Biochim. Biophys. Acta 455*, 322–331.

Chen, R. F., & Bowman, R. L. (1965) *Science (Washington, D.C.) 147*, 729–32.

Chen, L. A., Dale, R. E., Roth, S., & Brand, L. (1977) *J. Biol. Chem. 252*, 2163–2169.

Davenport, L. (1981) Ph.D. Thesis, Salford University, U.K.

Davenport, L., & Brand, L. (1984) *Biophys. J. 45*, 330a.

Davenport, L., & Brand, L. (1986) *Biochemistry* (in press).

Davenport, L., Knutson, J. R., & Brand, L. (1983) *Biophys. J. 41*, 373a.

DeLuca, M., Brand, L., Cebula, T. A., Seliger, H. H., & Makula, A. F. (1971) *J. Biol. Chem. 246*, 6702–6704.

Dittmer, J. C., & Lester, R. L. (1964) *J. Lipid Res. 5*, 126–127.

Easter, J. H., DeToma, R. P., & Brand, L. (1973) *Biochem. Biophys. Res. Commun. 52*, 1086–1092.

Förster, Th. (1949a) *Naturwissenschaften 36*, 186–187.

Förster, Th. (1949b) *Z. Elecktrochem. 54*, 42–46.

Grinvald, A. (1976) *Anal. Biochem. 75*, 260–280.

Grinvald, A., & Steinberg, I. Z. (1974) *Anal. Biochem. 59*, 583–598.

Gutman, M., Nachliel, E., Gershon, E., & Ginger, R. (1983) *Eur. J. Biochem. 134*, 63–69.

Hauser, H. O. (1971) *Biochem. Biophys. Res. Commun. 45*, 1049–1055.

Huang, C.-H. (1969) *Biochemistry 8*, 344–351.

Ireland, J. F., & Wyatt, P. A. H. (1976) *Adv. Phys. Org. Chem. 12*, 131–221.

Knight, A. E. W., & Selinger, B. K. (1971) *Spectrochim. Acta Part A 27A*, 1223.

Knutson, J. R., Walbridge, D. G., & Brand, L. (1982) *Biochemistry 21*, 4671–4679.

Knutson, J. R., Beechem, J. M., & Brand, L. (1983) *Chem. Phys. Lett. 102*, 501–507.

Laws, W. R., & Brand, L. (1979) *J. Phys. Chem. 83*, 795–802.

Loken, M. R., Hayes, J. W., Gohlke, J. R., & Brand, L. (1972) *Biochemistry 11*, 4779–4786.

McClare, C. W. F. (1971) *Anal. Biochem. 39*, 527–532.

Newman, G. C., & Huang, C.-H. (1975) *Biochemistry 14*, 3363–3369.

Örstan, A., Lulka, M. F., Eide, B., Petra, P. H., & Ross, J. B. A. (1986) *Biochemistry* (in press).

Paoletti, J., & LePecq, J.-B. (1969) *Anal. Biochem. 31*, 33–41.

Parker, C. A., & Rees, W. T. (1960) *Analyst (London) 85*, 587–600.

Selinger, B. K., & Harris, C. M. (1983) in *Time-Resolved Fluorescence Spectroscopy in Biochemistry and Biology* (Cundall, R. B., & Dale, R. E., Eds.) p 729, Plenum, New York.
Slaunwhite, W. R., Jr., Engel, L. L., Olmsted, P. C., & Carter, P. (1951) *J. Biol. Chem. 191*, 627–631.
Spencer, R. D., & Weber, G. (1970) *J. Chem. Phys. 52*, 1654–1663.
Weinreb, A., & Werner, A. (1974) *Photochem. Photobiol. 20*, 313–321.
Weinreb, A., Werner, A., & Kalman, Z. H. (1977) *Photochem. Photobiol. 26*, 567–572.
Weller, A. (1955) *Z. Phys. Chem. (Munich) 3*, 238–254.
Weller, A. (1958a) *Z. Phys. Chem. (Munich) 15*, 438–453.
Weller, A. (1958b) *Z. Phys. Chem. (Munich) 17*, 224–245.
Weller, A. (1961) *Prog. React. Kinet. 1*, 189–214.

Spontaneous Transmembrane Insertion of Membrane Proteins into Lipid Vesicles Facilitated by Short-Chain Lecithins†

Norbert A. Dencher
Biophysics Group, Department of Physics, Freie Universität Berlin, Arnimallee 14, D-1000 Berlin 33, FRG
Received September 25, 1985

ABSTRACT: Functional reconstitution of the membrane protein bacteriorhodopsin into lipid vesicles is achieved by mixing aqueous suspensions of long-chain lecithins and purple membrane with the short-chain lecithin diheptanoylphosphatidylcholine (20 mol % of total lipid). The membrane protein is transmembranously inserted in the lipid bilayer of the vesicle and highly active as a light-energized proton pump. This rapid, easy, and gentle procedure might allow functional reconstitution of other membrane systems and isolated membrane proteins as well.

Reconstituted protein–lipid vesicle systems are one of the most successful tools for the investigation of the structure and function of membrane proteins. Either the properties of the membrane protein of interest can be studied directly in these cell-like vesicles by means of various biochemical and biophysical techniques or the reconstituted vesicles are used as starting material for the formation of planar lipid bilayers containing transmembrane proteins suitable for electrical methods. A variety of approaches have been previously developed for functional reconstitution of membrane proteins into lipid vesicles [for recent reviews, see Racker (1979), Montal et al. (1981), and Eytan (1982)]. These approaches usually comprise at least one step which may be harmful for the membrane protein to various degrees, e.g., prolonged sonication, solubilization by and subsequent removal of detergents, and freezing and thawing. A reconstitution procedure avoiding any harmful treatment would obviously be an advantage, especially if it is easy and fast in addition. Recently, Gabriel and Roberts (1984) described a technique for spontaneously forming unilamellar lipid vesicles by mixing aqueous suspensions of long-chain lecithins (fatty acid chain lengths of 14 carbons or longer) with small amounts of micellar synthetic short-chain lecithins (chain lengths of 6–8 carbons). In the present report, it is shown that this technique is also an easy, rapid, and gentle way for successful membrane protein reconstitution. Bacteriorhodopsin (BR)[1] in the purple membrane (PM) of *Halobacterium halobium* is used as a model system in combination with different long-chain lecithins to demonstrate this fact. PM can be isolated without the use of detergents in pure form and contains as the sole protein the light-driven H^+ pump BR, which is only associated with seven native lipids. BR represents one of the best characterized transmembrane proteins, and its structural and functional properties can be easily monitored during reconstitution. In addition, several reconstitution procedures have been applied to BR (all of which require harsh treatments such as detergents, prolonged sonication, freeze–thawing, etc.) and therefore can be compared with the one under investigation (Hwang & Stoeckenius, 1977; Racker, 1979; Racker et al., 1979; Casadio & Stoeckenius, 1980; van Dijck et al., 1981; Heyn & Dencher, 1982; Rigaud et al., 1983). Upon mixing all constituents, i.e., PM, long-chain lecithins (DMPC, DPPC, and SBPL), and short-chain lecithins (diheptanoyl-PC), stable BR–lipid vesicles are spontaneously formed, which are active in light-energized H^+ translocation. Transmembrane insertion of BR into the lipid bilayer is verified by means of density gradient centrifugation, circular dichroism (CD) measurements, and vectorial H^+ transport. Reconstitution efficiency and general properties of the vesicles depend on the physical and chemical state of the long-chain lecithins. Since the novel method described allows functional transmembrane insertion of BR into lipid vesicles, future work might prove its ability for successful reconstitution of other membrane systems and isolated membrane proteins as well.

Experimental Procedures

Materials. DMPC and DPPC were obtained from Fluka and showed only one spot in thin-layer chromatography. DHPC and SBPL were purchased from Sigma. SBPL was purified by the procedure of Kagawa and Racker (1971). PM isolated from *Halobacterium halobium* S9 showed a single

† This research was supported by the Deutsche Forschungsgemeinschaft (SFB 312/B4, Heisenberg Grant De 300/1).

[1] Abbreviations: BR, bacteriorhodopsin; PM, purple membrane; DMPC, dimyristoylphosphatidylcholine; DPPC, dipalmitoylphosphatidylcholine; SBPL, soybean phospholipid(s); DHPC, diheptanoylphosphatidylcholine; CD, circular dichroism; $NaDodSO_4$, sodium dodecyl sulfate.

0006-2960/86/0425-1195$01.50/0